Observation of several sources of CP violation in $B^+ \rightarrow \pi\pi\pi$ decays

Alvaro Gomes, on behalf of LHCb collaboration

Conference on Flavour Physics and CP Violation FPCP 2019
May 6-10 , 2019

Overview

LHCb Collaboration, Phys. Rev. D90, 112004 (2014)

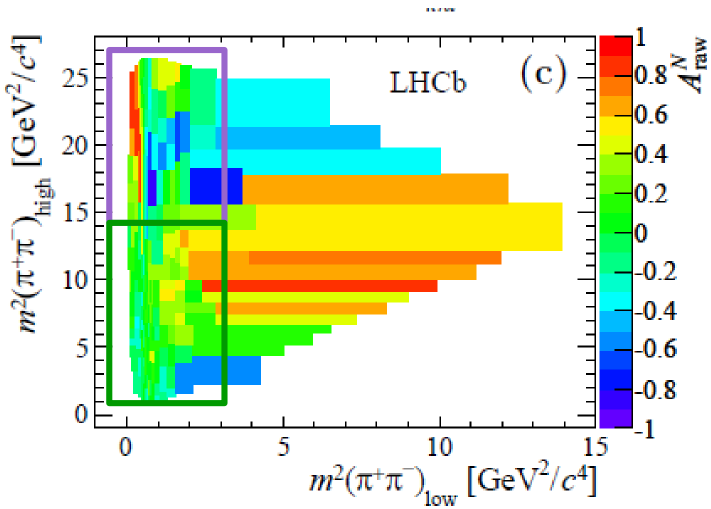

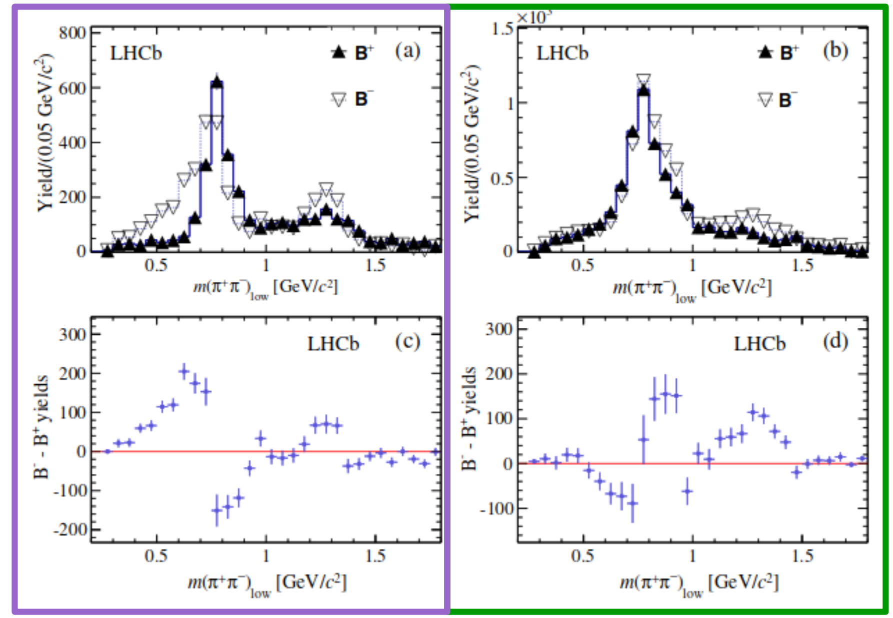

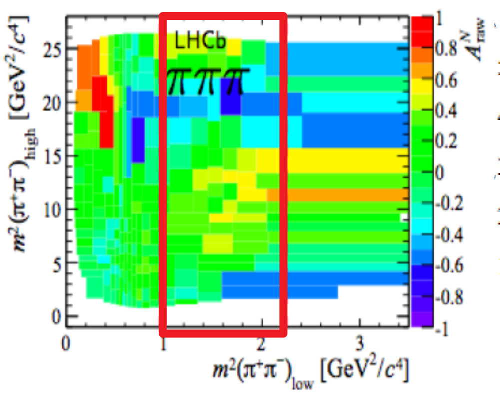

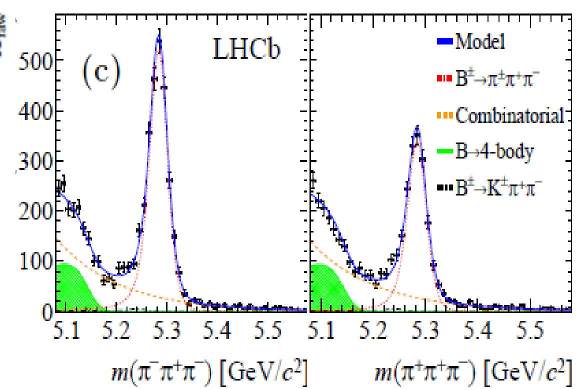

Decay	N_S	A_{CP}
$B^\pm \to \pi^\pm\pi^+\pi^-$	4329 ± 76	$+0.172 \pm 0.021 \pm 0.015 \pm 0.007$

- Rich interference pattern leading to positive and negative CP asymmetries.
- Large CP asymmetry observed in the rescattering region m(ππ) between 1.0 and 1.5 GeV/c^2. J.R. Pelaez and F. J. Yndurain Phys. Rev. D71,074016 (2005)

Overview

- large CP asymmetries observed in regions of the phase space :
  - some cancel out, e.g. within the $\rho(770)$ region.
  - some do not cancel: CPV must be compensated to ensure CPT
- $KK \leftrightarrow \pi\pi$ rescattering is a way to ensure CPT.
  - $B^+ \to \pi KK$ and $B^+ \to \pi\pi\pi$ are connected.
    - $B^+ \to \pi KK$ CP asymmetries reported at LHCb-PAPER-2018-051 and will be covered by M. Sevior in B hadronic 1 section tomorrow (May 8th) 12pm.
  - This constraint includes all other coupled channels.
- the CP asymmetries in phase space may be a manifestation of:
  - Penguin/tree interference with different strong phases.
  - Resonance dynamic (which also gives a strong phase difference).
  - $KK \leftrightarrow \pi\pi$ rescattering.

The amplitude analysis of the four channels will help elucidate and verify some **hypotheses**

$B^+ \to \pi\pi\pi$ sample

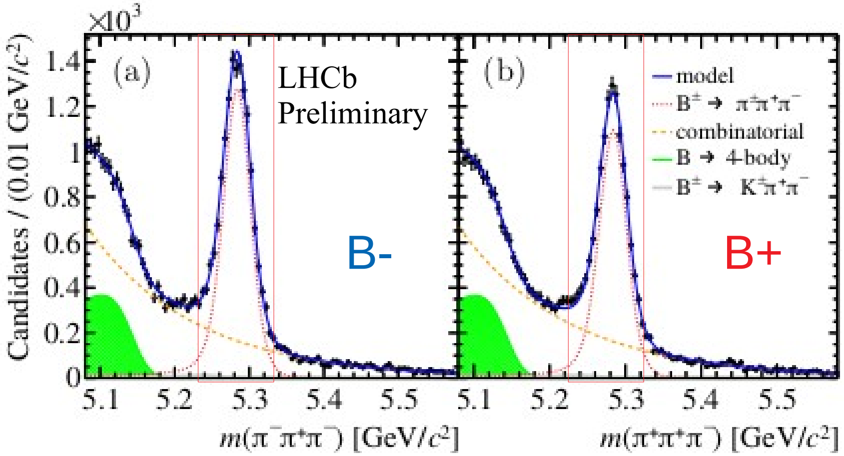

Parameter	Value
Signal yield	$20\,594 \pm 1\,569$
Combinatorial background yield	$4\,409 \pm 1\,634$
$B^+ \to K^+\pi^+\pi^-$ background yield	143 ± 11
Combinatorial background asymmetry	$+0.005 \pm 0.010$
$B^+ \to K^+\pi^+\pi^-$ background asymmetry	$+0.000 \pm 0.008$

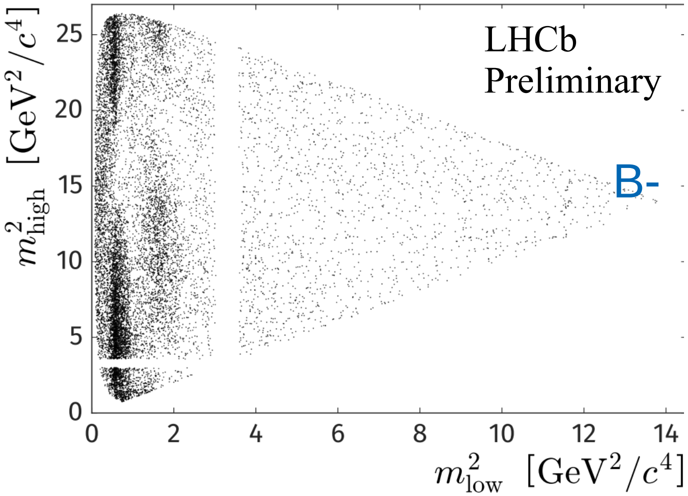

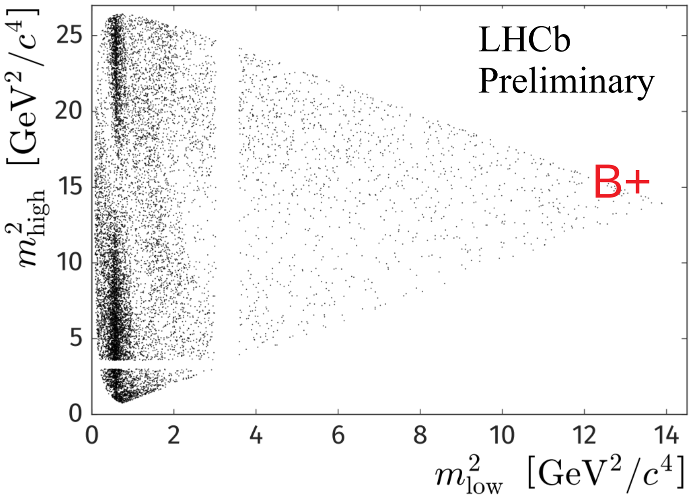

- Sample correspond to 3fb^{-1} from Run 1.

$B^+ \to \pi\pi\pi$ sample

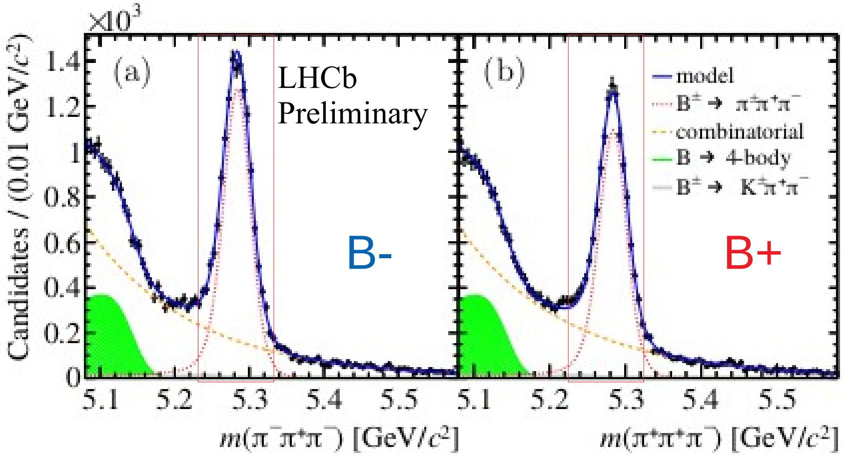

Parameter	Value
Signal yield	$20\,594 \pm 1\,569$
Combinatorial background yield	$4\,409 \pm 1\,634$
$B^+ \to K^+\pi^+\pi^-$ background yield	143 ± 11
Combinatorial background asymmetry	$+0.005 \pm 0.010$
$B^+ \to K^+\pi^+\pi^-$ background asymmetry	$+0.000 \pm 0.008$

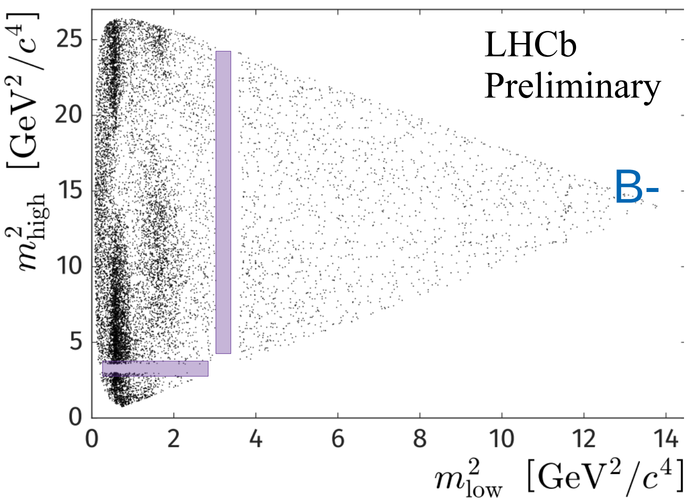

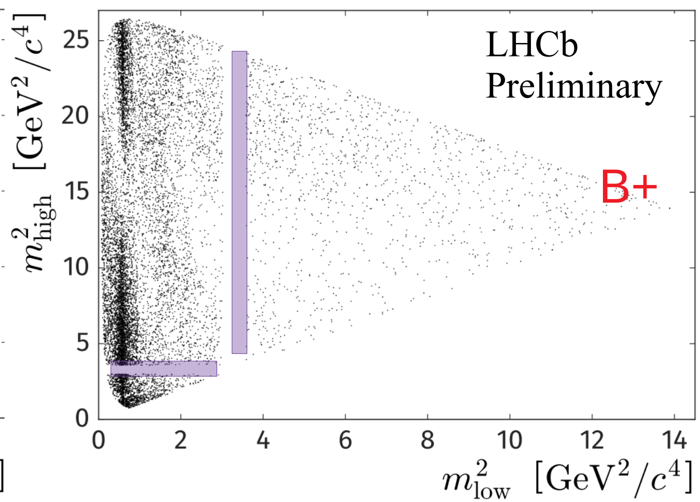

- Sample correspond to 3fb^{-1} from Run 1.
- Charm veto.

$B^+ \rightarrow \pi\pi\pi$ sample

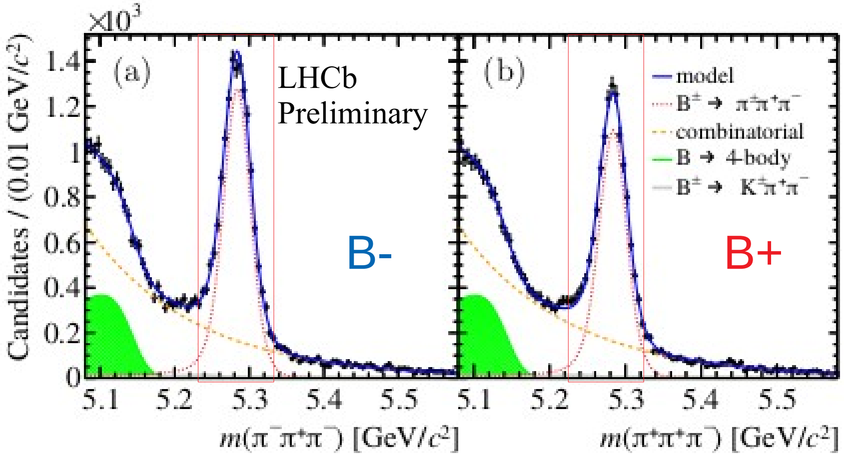

Parameter	Value
Signal yield	$20\,594 \pm 1\,569$
Combinatorial background yield	$4\,409 \pm 1\,634$
$B^+ \to K^+\pi^+\pi^-$ background yield	143 ± 11
Combinatorial background asymmetry	$+0.005 \pm 0.010$
$B^+ \to K^+\pi^+\pi^-$ background asymmetry	$+0.000 \pm 0.008$

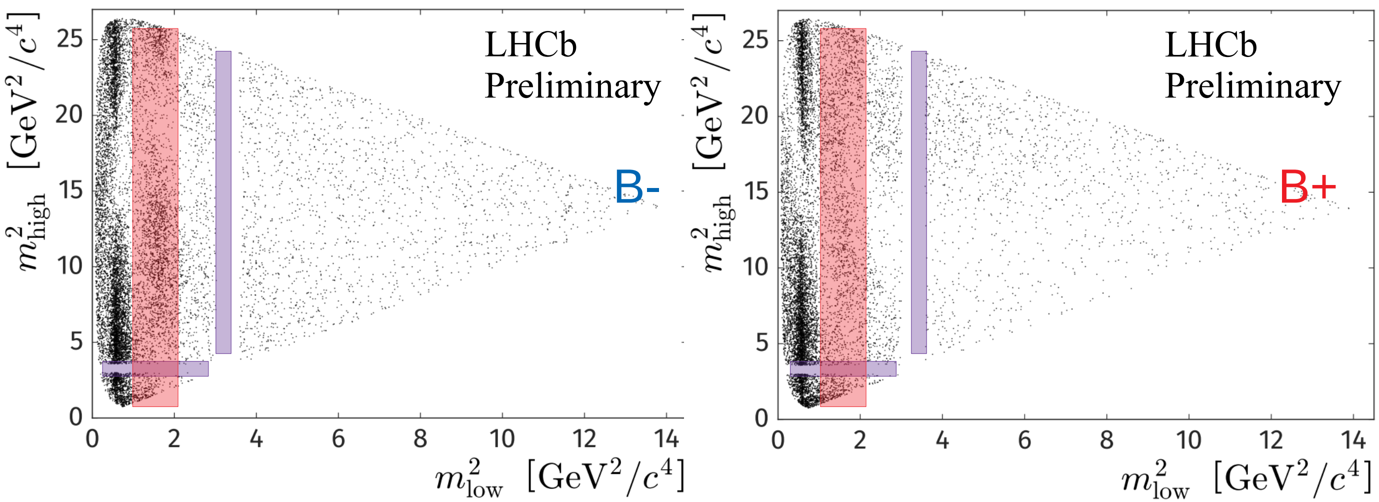

- Sample correspond to 3fb^{-1} from Run 1.
- Charm veto.
- $f_2(1270)$ region.

$B^+ \to \pi\pi\pi$ sample

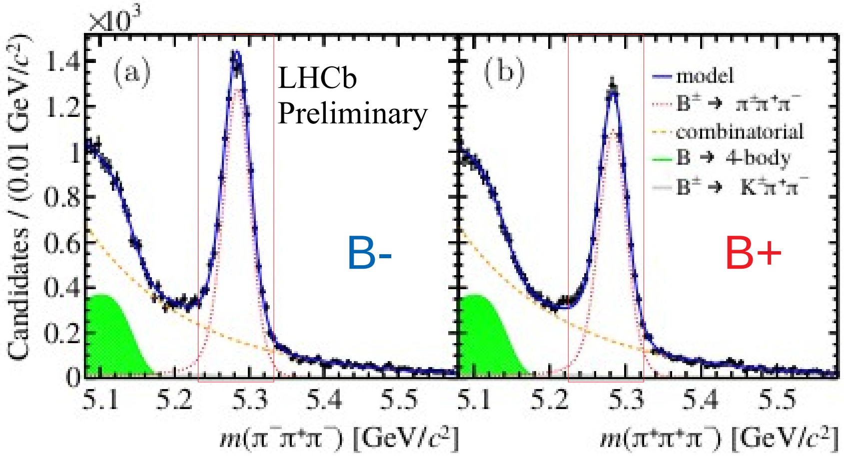

Parameter	Value
Signal yield	$20\,594 \pm 1\,569$
Combinatorial background yield	$4\,409 \pm 1\,634$
$B^+ \to K^+\pi^+\pi^-$ background yield	143 ± 11
Combinatorial background asymmetry	$+0.005 \pm 0.010$
$B^+ \to K^+\pi^+\pi^-$ background asymmetry	$+0.000 \pm 0.008$

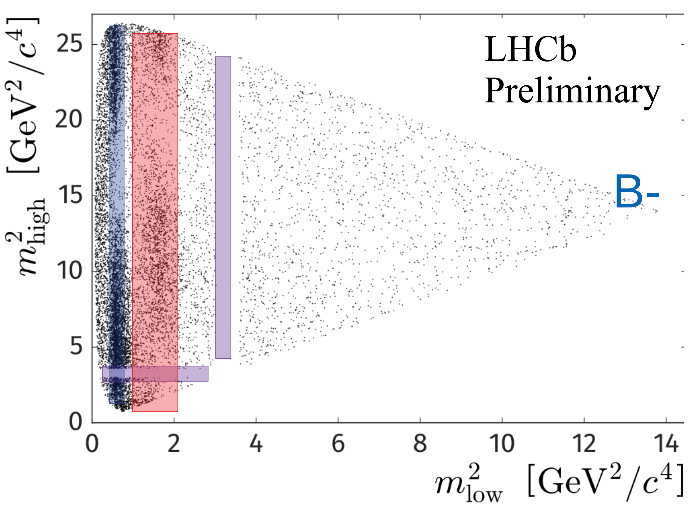

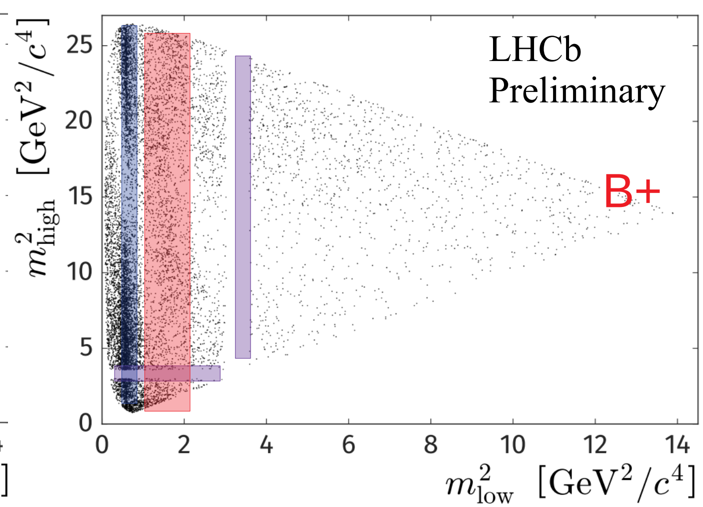

- Sample correspond to $3\,\text{fb}^{-1}$ from Run 1.
- Charm veto.
- $f_2(1270)$ region.
- $\rho(770)$ region.

$B^+ \to \pi\pi\pi$ sample

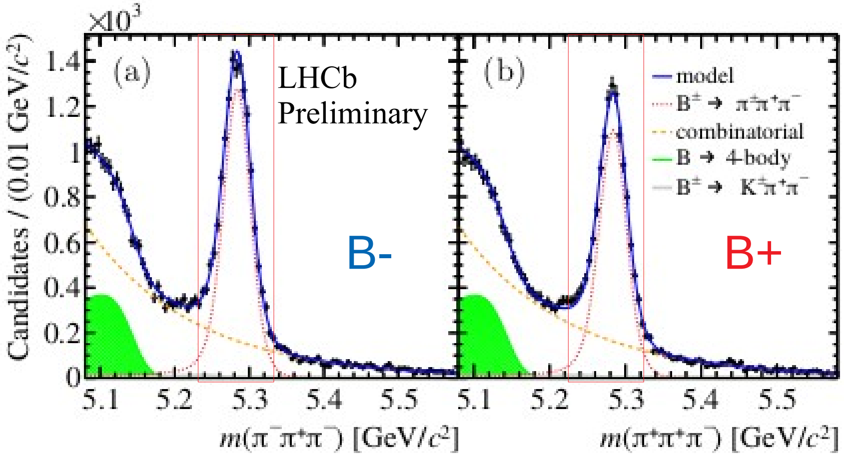

Parameter	Value
Signal yield	$20\,594 \pm 1\,569$
Combinatorial background yield	$4\,409 \pm 1\,634$
$B^+ \to K^+\pi^+\pi^-$ background yield	143 ± 11
Combinatorial background asymmetry	$+0.005 \pm 0.010$
$B^+ \to K^+\pi^+\pi^-$ background asymmetry	$+0.000 \pm 0.008$

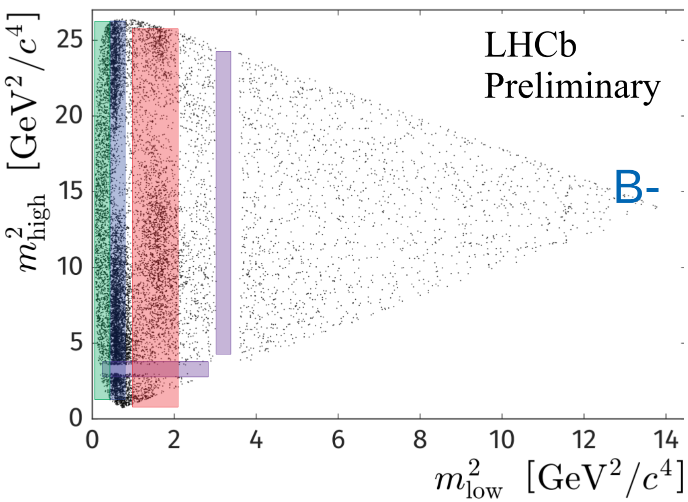

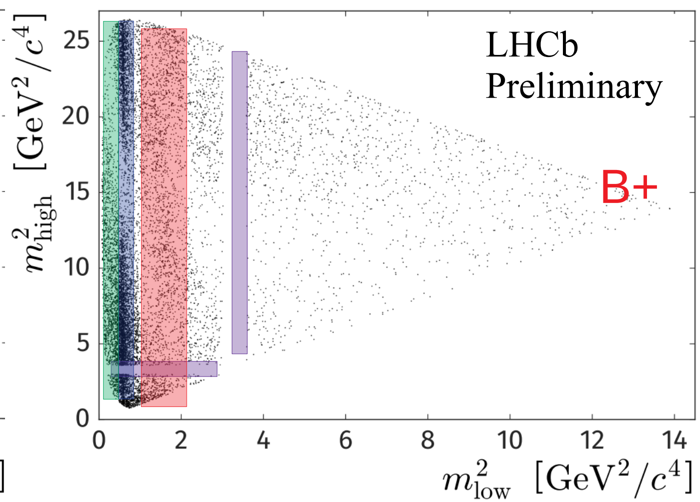

- Sample correspond to 3fb^{-1} from Run 1.
- Charm veto.
- $f_2(1270)$ region.
- $\rho(770)$ region.
- low scalar $m(\pi\pi)$.

$B^+ \to \pi\pi\pi$ sample

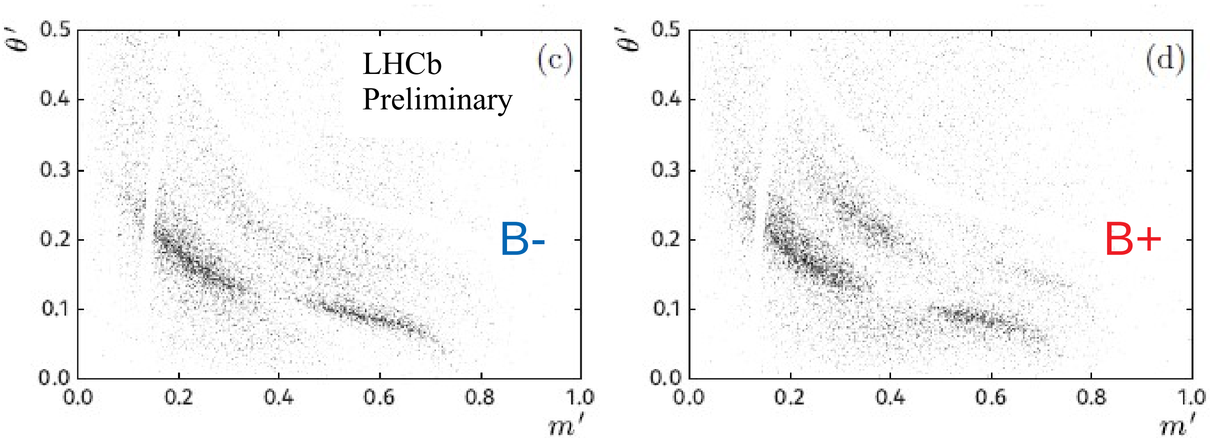

$$m' \equiv \frac{1}{\pi}\cos^{-1}\left(2\frac{m(\pi^+\pi^+) - m(\pi^+\pi^+)^{\min}}{m(\pi^+\pi^+)^{\max} - m(\pi^+\pi^+)^{\min}} - 1\right)$$

$$\theta' \equiv \frac{1}{\pi}\theta(\pi^+\pi^+),$$

- $m(\pi\pi)^{min}$ and $m(\pi\pi)^{max}$ represents the kinematic limits permitted in 3π decays
- $\theta(\pi\pi)$ is the angle between π^+ and π^- in the $\pi^+\pi^+$ rest frame

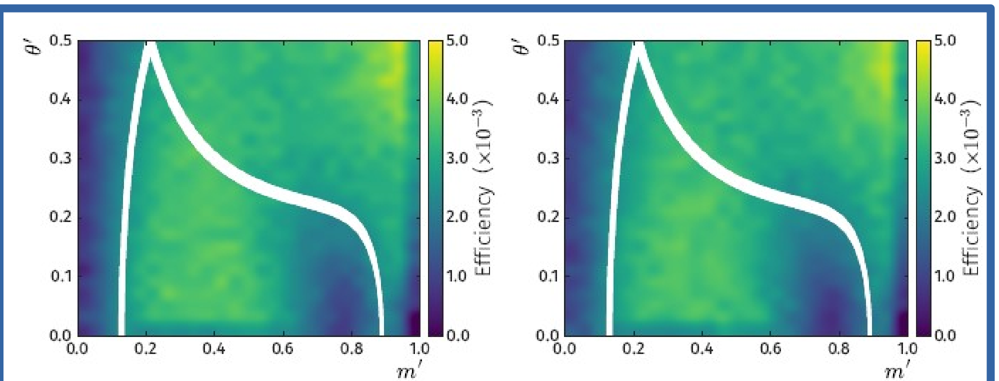

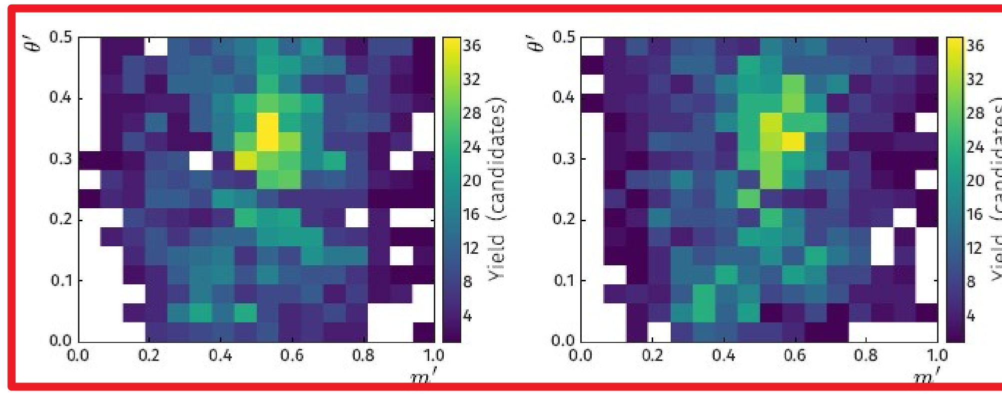

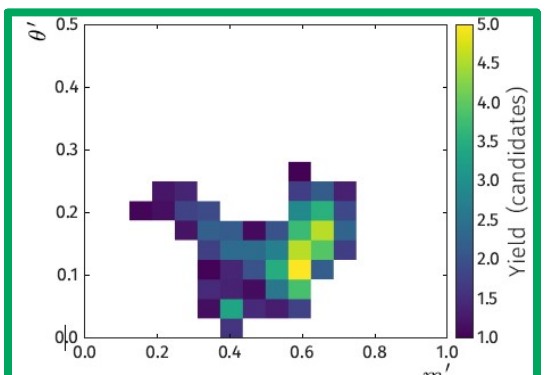

- Signal efficiency.
- Combintorial background models.
- $B \to K\pi\pi$ background model.

Amplitude analysis of $B^+ \to \pi\pi\pi$

- Isobar model for all non S-wave contributions

$$A^+(m_{13}^2, m_{23}^2) = \sum_j^N A_j^+(m_{13}^2, m_{23}^2) = \sum_j^N c_j^+ F_j(m_{13}^2, m_{23}^2)$$
$$A^-(m_{13}^2, m_{23}^2) = \sum_j^N A_j^-(m_{13}^2, m_{23}^2) = \sum_j^N c_j^- F_j(m_{13}^2, m_{23}^2)$$

  - Coherent sum of intermediate contributions
  - c_j complex coeficients extracted from the fit to B+ and B- data

- Quasi-two-body CP asymmetry in j: $A_{CP}^j = \frac{|A_j^-|^2 - |A_j^+|^2}{|A_j^-|^2 + |A_j^+|^2}$

- Fit fraction: $F_j^\pm = \frac{\int_{DP} |A_j^\pm(m_{13}^2, m_{23}^2)|^2 dm_{13}^2 dm_{23}^2}{\int_{DP} |A^\pm(m_{13}^2, m_{23}^2)|^2 dm_{13}^2 dm_{23}^2}$

Amplitude analysis of $B^+ \to \pi\pi\pi$

- S-wave with three different approaches:
  - Isobar: pole with floating mass and width J.A. Oller Phys. Rev. D71, 054030 (2005) + KK ↔ ππ rescattering contribution I. Bediaga et al. Phys. Rev. D89, 094013 (2014).
  - K-matrix: includes rescattering couplings to 5 intermediate states (ππ, KK, ηη, ηη', 4π) resulting in a single two body unitary amplitude. V. V. Anisovich et al. Eur. Phys. J. A16, 229 (2003)

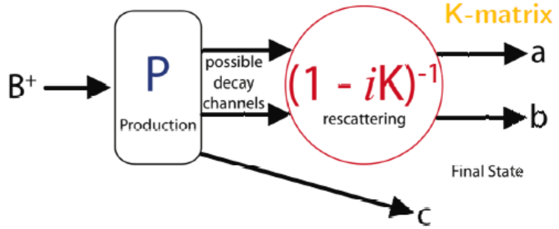

  - Quasi Model Independent(QMI): fit magnitude and phase in bins of the Dalitz plot for B+ and B-. E791 Collaboration Phys. Rev. D73, 032004 (2006)

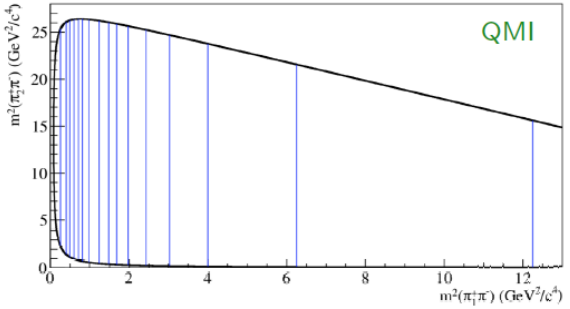

- **All three approaches obtain similar non S-wave results.**

CP asymmetry in the ρ(770) region

- No CP asymmetry in the ρ(770) region as can be seen in the m_{low} projections:

ρ(770) - ω(782) mixing well described!

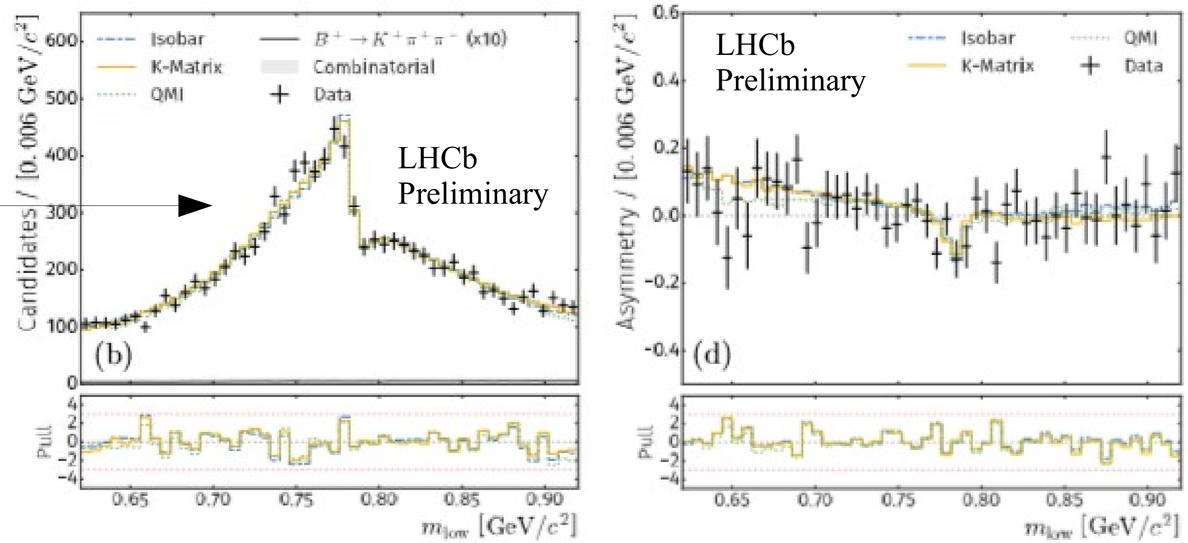

- Large CP asymmetry in the scalar - ρ(770) interference observed in projections of the helicity angle around the ρ(770) mass:

25σ significance

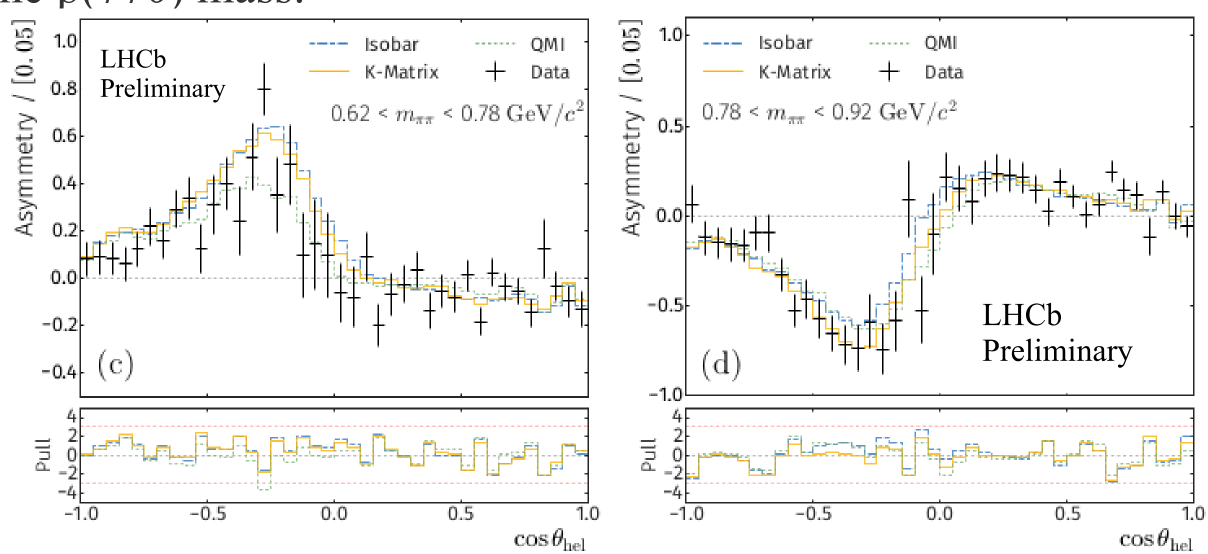

CP asymmetry in the $f_2(1270)$ region

- We observed a large positive quasi-two-body CP asymmetry in the $f_2(1270)$ region (A_{cp} in %):

Component	Isobar	K-matrix	QMI
$f_2(1270)$	$+46.8 \pm 6.1 \pm 3.6 \pm 4.4$	$+42.8 \pm 4.1 \pm 2.1 \pm 8.9$	$+37.6 \pm 4.4 \pm 6.0 \pm 5.2$

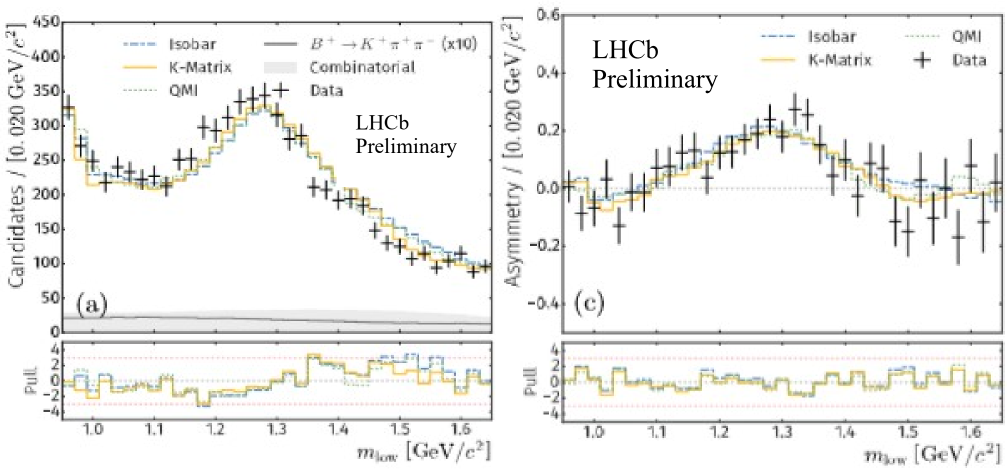

- First CPV observation in any process involving a tensor resonance.

10σ significance

CP asymmetry in the $f_2(1270)$ region

- We observed a large positive quasi-two-body CP asymmetry in the $f_2(1270)$ region (A_{cp} in %):

Component	Isobar	K-matrix	QMI
$f_2(1270)$	$+46.8 \pm 6.1 \pm 3.6 \pm 4.4$	$+42.8 \pm 4.1 \pm 2.1 \pm 8.9$	$+37.6 \pm 4.4 \pm 6.0 \pm 5.2$

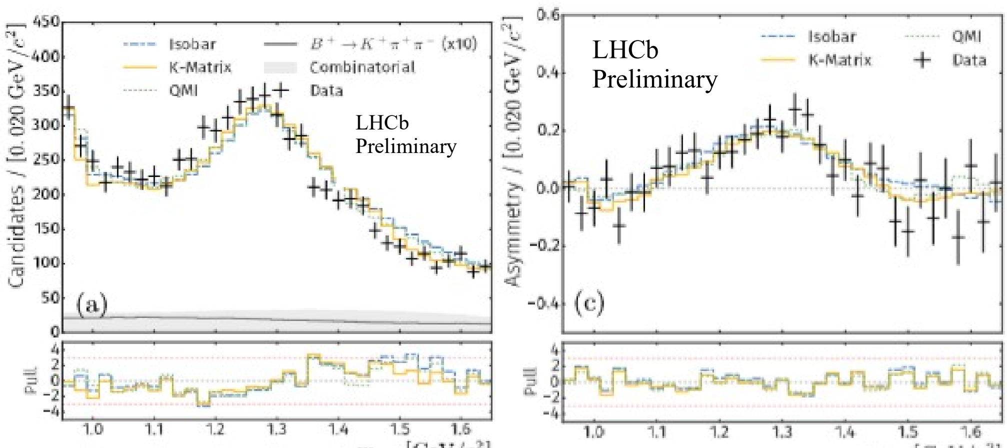

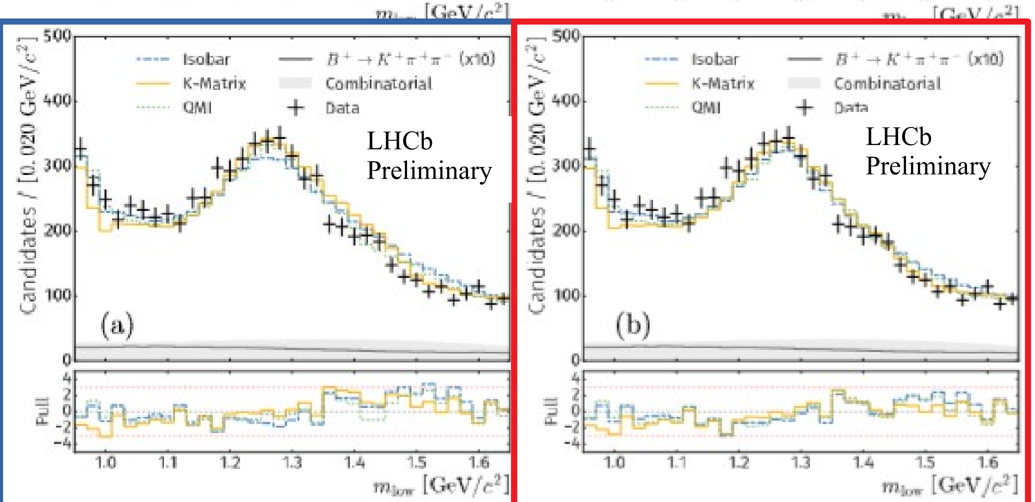

- First CPV observation in any process involving a tensor resonance.

10σ significance

- Fit to data not perfect:
  - Fit with $f_2(1270)$ free parameters
  - Fit including an additional spin-2 component.

CP asymmetry in the S-wave

- CP asymmetry in the S-wave:

Component	Isobar	K-matrix	QMI
S-wave	$+14.4 \pm 1.8 \pm 2.1 \pm 1.9$	$+15.8 \pm 2.6 \pm 2.1 \pm 6.9$	$+15.0 \pm 2.7 \pm 4.2 \pm 7.0$

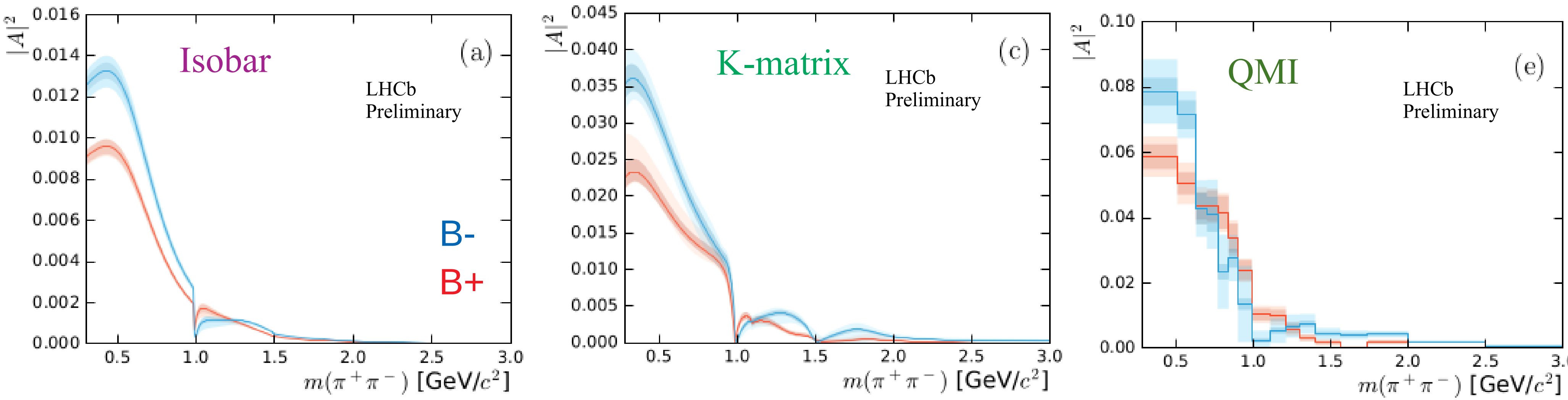

LHCb-PAPER-2019-017 and LHCb-PAPER-2019-018 in preparation.

CP asymmetry in the S-wave

- CP asymmetry in the S-wave:

Component	Isobar	K-matrix	QMI
S-wave	$+14.4 \pm 1.8 \pm 2.1 \pm 1.9$	$+15.8 \pm 2.6 \pm 2.1 \pm 6.9$	$+15.0 \pm 2.7 \pm 4.2 \pm 7.0$

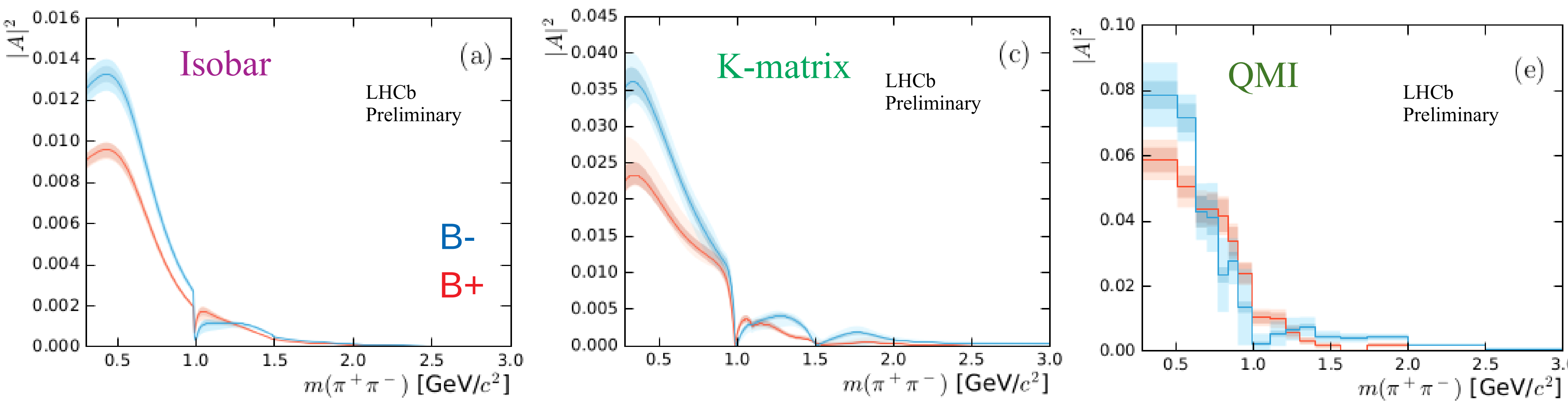

- Remarkably good agreement between all three approaches.

CP asymmetry in the S-wave

- CP asymmetry in the S-wave:

Component	Isobar	K-matrix	QMI
S-wave	$+14.4 \pm 1.8 \pm 2.1 \pm 1.9$	$+15.8 \pm 2.6 \pm 2.1 \pm 6.9$	$+15.0 \pm 2.7 \pm 4.2 \pm 7.0$

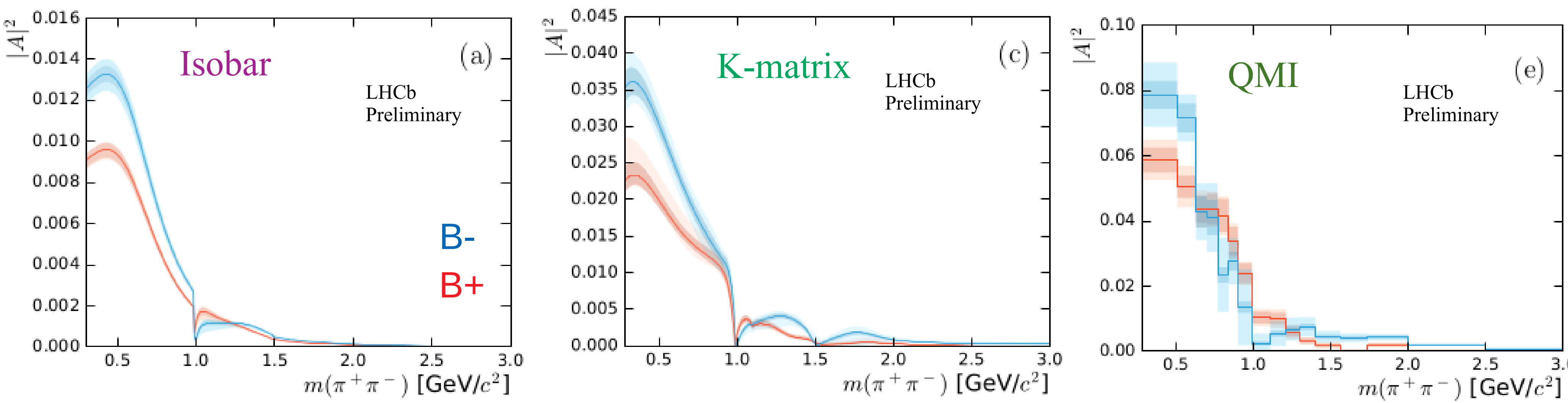

- Remarkably good agreement between all three approaches.
- Positive CP asymmetry at low m(ππ) that flips sign around the opening of the KK threshold (1GeV/c²).

10σ significance

Results for $B^+ \rightarrow \pi\pi\pi$

Contribution	Fit fraction (%)	A_{CP} (10^{-2})	B^+ phase (°)	B^- phase (°)
Isobar Model				
$\rho(770)^0$	55.5 ± 0.6 ± 1.7	+0.7 ± 1.1 ± 2.2	—	—
$\omega(782)$	0.50 ± 0.03 ± 0.05	−4.8 ± 6.4 ± 9.4	−19 ± 6 ± 1	+8 ± 16 ± 1
$f_2(1270)$	9.0 ± 0.3 ± 1.4	+46.8 ± 5.5 ± 5.8	+5 ± 3 ± 12	+53 ± 2 ± 12
$\rho(1450)^0$	5.2 ± 0.3 ± 1.5	−12.9 ± 6.4 ± 29.7	+127 ± 4 ± 21	+154 ± 4 ± 6
$\rho_3(1690)^0$	0.5 ± 0.1 ± 0.2	−80.1 ± 11.7 ± 22.9	−26 ± 7 ± 14	−47 ± 18 ± 25
S-wave	25.4 ± 0.5 ± 1.3	+14.4 ± 1.8 ± 3.3	—	—
rescatt	1.4 ± 0.1 ± 0.4	+44.7 ± 9.0 ± 16.6	−35 ± 6 ± 10	−4 ± 4 ± 25
σ	25.2 ± 0.6 ± 1.1	+16.0 ± 2.0 ± 3.2	+115 ± 2 ± 14	+179 ± 1 ± 95
K-Matrix				
$\rho(770)^0$	56.5 ± 0.7 ± 3.4	+4.2 ± 1.5 ± 6.4	—	—
$\omega(782)$	0.47 ± 0.04 ± 0.03	−6.2 ± 8.4 ± 9.8	−15 ± 6 ± 4	+8 ± 7 ± 4
$f_2(1270)$	9.3 ± 0.4 ± 2.5	+42.8 ± 4.1 ± 9.1	+19 ± 4 ± 18	+80 ± 3 ± 17
$\rho(1450)^0$	10.5 ± 0.7 ± 4.6	+9.0 ± 6.0 ± 47.0	+155 ± 5 ± 29	−166 ± 4 ± 51
$\rho_3(1690)^0$	1.5 ± 0.1 ± 0.4	−35.7 ± 10.8 ± 36.9	+19 ± 8 ± 34	+5 ± 8 ± 46
S-wave	25.7 ± 0.6 ± 3.0	+15.8 ± 2.6 ± 7.2	—	—
QMI				
$\rho(770)^0$	54.8 ± 1.0 ± 2.2	+4.4 ± 1.7 ± 2.8	—	—
$\omega(782)$	0.57 ± 0.10 ± 0.17	−7.9 ± 16.5 ± 15.8	−25 ± 6 ± 27	−2 ± 7 ± 11
$f_2(1270)$	9.6 ± 0.4 ± 4.0	+37.6 ± 4.4 ± 8.0	+13 ± 5 ± 21	+68 ± 3 ± 66
$\rho(1450)^0$	7.4 ± 0.5 ± 4.0	−15.5 ± 7.3 ± 35.2	+147 ± 7 ± 152	−175 ± 5 ± 171
$\rho_3(1690)^0$	1.0 ± 0.1 ± 0.5	−93.2 ± 6.8 ± 38.9	+8 ± 10 ± 24	+36 ± 26 ± 46
S-wave	26.8 ± 0.7 ± 2.2	+15.0 ± 2.7 ± 8.1	—	—

Quasi-two-body CP asymmetry consistent with zero

Conclusions

- First LHCb amplitude analysis of the $B^+ \to \pi\pi\pi$ decays.
- Large CPV due to the S and P-wave interference.
  - Quasi-two-body CP asymmetry in $\rho(770)$ is consistent with zero.
- All three approaches observe CPV in the S-wave.
- Large quasi-two-body CP asymmetry in the $f_2(1270)$ component.
- Evidence of CP asymmetry related to the rescattering component.
  - KK $\leftrightarrow$ pipi rescattering plays an important role.
  - Further improvements needed to better describe the rescattering term.

    J. R. Pelaez, A. Rodas, arXiv:1807.04543 (2018). To appear on Eur. Phys. J. C.
- All results presented here will be published in two imminent papers.

LHCb run 2 data to be analyzed $\to$ 5 times larger data sample!

backup

- List of systematics: Isobar

Category	$\rho(770)^0$	$\omega(782)$	$f_2(1270)$	$\rho(1450)^0$	$\rho_3(1690)^0$	S-wave	Rescattering	σ
B mass fit	0.12	0.10	0.89	0.40	4.19	0.58	4.20	0.54
Efficiency								
Simulation sample size	0.34	0.71	0.61	0.92	1.24	0.36	1.00	0.35
Binning	0.27	0.87	0.23	1.19	0.52	0.28	1.43	0.22
L0 Trigger	0.02	0.37	0.17	0.31	0.28	0.14	0.32	0.19
Combinatorial	0.40	0.50	1.02	3.06	5.75	0.75	3.16	0.75
$B^+ \to K^+\pi^+\pi^-$	< 0.01	0.01	0.02	0.03	0.05	0.01	0.04	0.01
Fit bias	1.07	6.51	3.25	6.10	11.36	1.79	8.59	1.73
Total experimental	1.23	6.64	3.58	7.01	13.47	2.08	10.23	2.01
Amplitude model								
Resonance properties	0.20	0.53	0.55	2.66	5.58	0.41	1.58	0.29
Barrier factors	0.18	0.95	0.80	3.84	1.56	1.27	0.34	1.25
Alternative lineshapes								
$f_2(1270)$	0.11	0.10	0.82	0.30	4.05	0.49	4.07	0.45
$f_2(1430)$	0.02	0.04	2.84	1.76	12.05	0.98	6.39	1.05
$\rho(1700)^0$	1.49	0.81	0.75	27.78	4.57	0.73	6.32	0.66
Isobar specifics								
σ from PDG	0.01	3.26	2.97	21.83	19.04	0.11	12.9	0.53
Rescattering	0.02	0.14	0.81	0.19	1.97	0.29	1.24	0.17
Total model	1.52	3.54	4.44	35.68	24.13	1.90	16.37	1.92
Statistical uncertainty	1.07	6.51	6.10	3.25	11.36	1.79	8.59	1.73

backup

- List of systematics: K-matrix

Category	$\rho(770)^0$	$\omega(782)$	$f_2(1270)$	$\rho(1450)^0$	$\rho_3(1690)^0$	S-wave
B mass fit	1.97	0.12	1.42	9.74	5.77	1.03
Efficiency						
Simulation sample size	0.22	0.88	0.73	0.97	1.34	0.42
Binning	1.53	5.48	0.15	2.89	1.72	1.54
L0 trigger	0.15	0.59	0.19	0.32	0.30	0.02
Combinatorial	0.61	0.60	1.31	3.45	5.82	0.93
$B^+ \to K^+\pi^+\pi^-$	0.01	0.03	0.03	0.04	0.12	0.03
Fit bias	0.02	0.04	0.24	0.85	0.40	0.36
Total experimental	2.60	5.60	2.09	10.81	8.49	2.13
Amplitude model						
Resonance properties	0.62	0.91	1.08	4.35	5.34	1.27
Barrier factors	1.97	3.54	0.04	12.53	2.79	3.50
Alternative lineshapes						
$f_2(1270)$	0.58	0.56	0.48	2.96	4.41	1.13
$f_2(1430)$	3.04	1.69	8.78	41.78	33.96	4.77
$\rho(1700)^0$	3.38	1.17	0.39	8.82	8.80	1.60
K-matrix specifics						
s^0_{prod}	2.08	4.42	0.20	3.42	0.98	2.41
K-matrix components	2.11	5.31	0.01	8.11	0.21	1.03
Total model	5.84	8.10	8.87	45.67	35.88	6.88
Statistical uncertainty	1.5	8.4	4.3	8.4	11.8	2.6

backup

- List of systematics: QMI

Category	$\rho(770)^0$	$\omega(782)$	$f_2(1270)$	$\rho(1450)^0$	$\rho_3(1690)^0$	S-wave
B mass fit	0.40	1.02	0.23	0.92	0.31	0.04
Efficiency						
Simulation sample size	0.54	1.59	2.29	1.19	0.67	0.46
Binning	0.26	1.46	0.25	1.31	0.87	0.24
L0 trigger	0.15	0.75	0.14	0.07	0.12	0.04
Combinatorial	0.91	3.05	1.96	10.99	2.88	2.72
$B^+ \to K^+\pi^+\pi^-$	0.01	0.04	0.11	0.33	0.30	0.07
Fit bias	1.92	13.45	5.14	8.24	7.07	2.86
Total experimental	2.29	14.20	6.04	14.25	8.00	4.17
Amplitude model						
Resonance properties	0.47	2.31	0.88	3.23	2.06	1.26
Barrier factors	0.17	3.39	1.99	12.01	3.03	5.12
Alternative lineshapes						
$f_2(1270)$	0.02	0.68	0.70	0.98	0.32	0.67
$f_2(1430)$	0.51	0.72	0.08	2.96	1.52	0.67
$\rho(1700)^0$	0.63	2.37	0.97	4.09	0.29	1.39
QMI specifics						
QMI bias	1.35	5.56	4.70	29.40	37.89	4.40
Total model	1.58	7.00	5.24	32.17	38.05	6.96
Statistical uncertainty	1.27	15.44	3.63	5.55	17.01	1.52

backup

- S-wave magnitude and phases

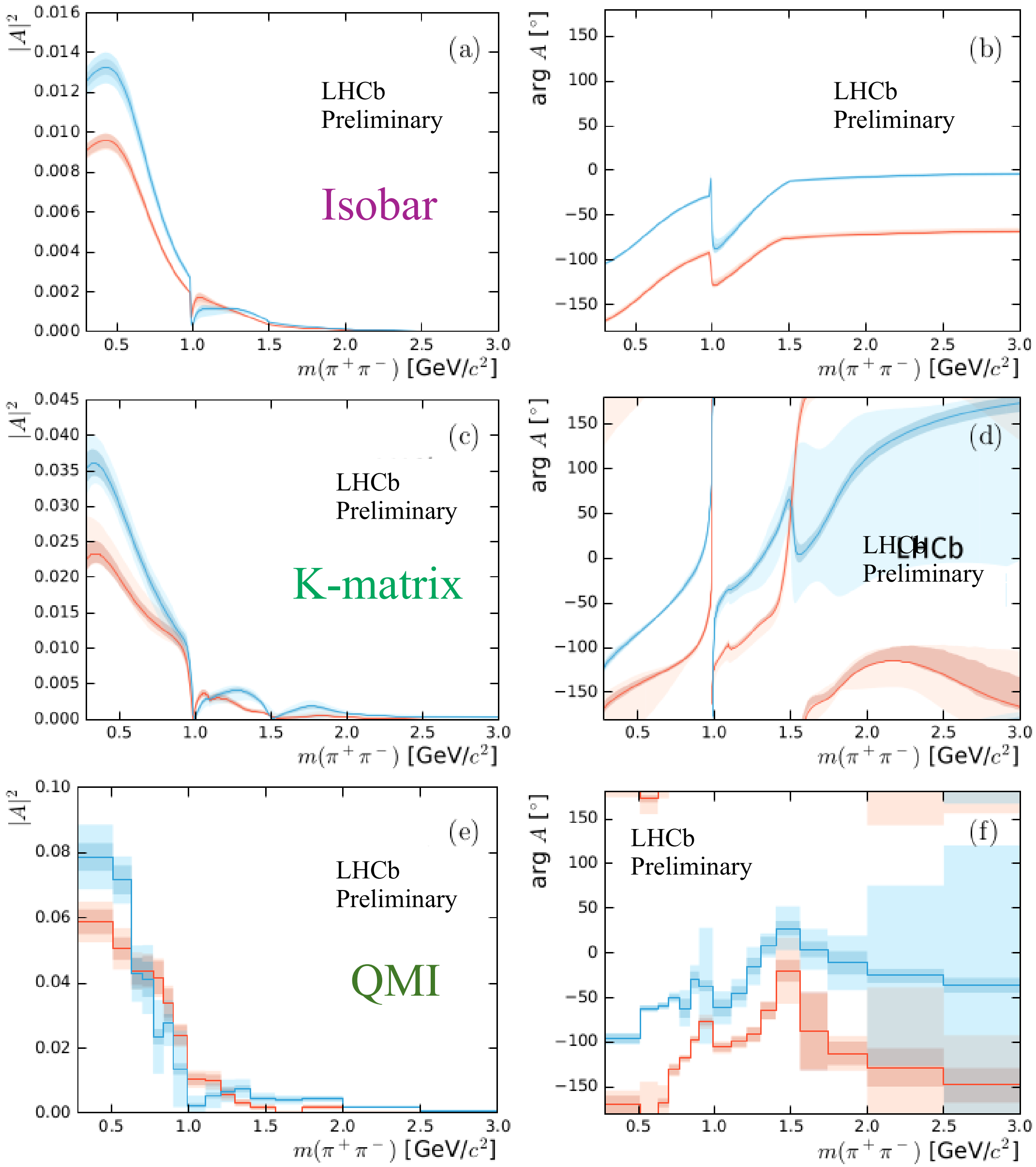

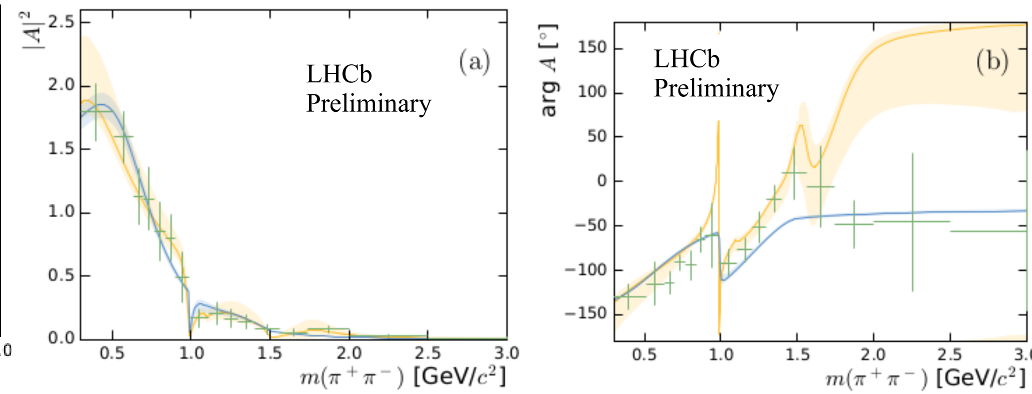

- For the combined plot:
  - Blue curve is the isobar S-wave
  - Amber curve is the K-matrix swave
  - Green points with error bars is the QMI s-wave

backup

- Argand for $f_2(1270)$ asymmetry